Supernova neutrino oscillations: A simple analytical approach

G.L. Fogli [1], E. Lisi [1], D. Montanino [2], and A. Palazzo [1]

[1] *Dipartimento di Fisica and Sezione INFN di Bari*
Via Amendola 173, 70126 Bari, Italy
[2] *Dipartimento di Scienza dei Materiali and Sezione INFN di Lecce*
Via Arnesano, 73100 Lecce, Italy

Abstract

Analyses of observable supernova neutrino oscillation effects require the calculation of the electron (anti)neutrino survival probability P_{ee} along a given supernova matter density profile. We propose a simple analytical prescription for P_{ee}, based on a double-exponential form for the crossing probability and on the concept of maximum violation of adiabaticity. In the case of two-flavor transitions, the prescription is shown to reproduce accurately, in the whole neutrino oscillation parameter space, the results of exact numerical calculations for generic (realistic or power-law) profiles. The analytical approach is then generalized to cover three-flavor transitions with (direct or inverse) mass spectrum hierarchy, and to incorporate Earth matter effects. Compact analytical expressions, explicitly showing the symmetry properties of P_{ee}, are provided for practical calculations.

PACS number(s): 14.60.Pq, 97.60.Bw

I. INTRODUCTION

Observable effects of supernova neutrinos in underground detectors represent a subject of intense investigation in astroparticle physics, both on general grounds (see the reviews in [1,2]) and in relation to the SN1987A event (see [3] for an updated analysis and bibliography). In particular, flavor oscillations in supernovae may shed light on the problem of neutrino masses and mixing, by means of the (potentially strong) associated matter effects (see, e.g., [1,4–6] for reviews of early works, and [7–20] for an incomplete list of recent studies). In particular, dramatic effects on oscillations have been predicted, related to the type of neutrino mass spectrum hierarchy and to Earth matter crossing.

Given the importance of supernova neutrino oscillations for both particle physics and astrophysics, it would be desirable to have a simple and complete description of the most important quantity involved in the calculations, namely, of the electron (anti)neutrino survival probability P_{ee}.[1] Approximate treatments of P_{ee} have been proposed in the literature to cover parts the parameter space in a piecewise fashion, e.g., by using either the adiabatic approximation or the so-called resonance condition (see [21,7,10,11] for recent examples), with inherent limitations in the range of applicability. In particular, it has been recently realized, first in the context of solar [22,23] and then of supernova [16,17] neutrinos, that the time-honored resonance condition cannot be meaningfully extended at large neutrino mixing. Thus, apart from brute-force numerical calculations of P_{ee} (see, e.g., [24,18–20]), a truly unified approach, valid in the whole three-flavor oscillation parameter space and applicable to generic supernova density profiles, seems still lacking in the literature, as far as we know.

In this work, we propose a simple, unified analytical approach to the calculation of P_{ee}, based on a double-exponential form for the crossing probability [25,26] and on the condition of maximum violation of adiabaticity [22,23] (replacing the popular resonance condition). In the case of two-flavor transitions (Sec. II), our prescription is shown to reproduce accurately the results of exact numerical calculations for generic (realistic or power-law) profiles, in the whole neutrino oscillation parameter space. The analytical approach is then generalized to cover three-flavor transitions with (direct or inverse) mass spectrum hierarchy (Sec. III), and to incorporate Earth matter effects (Sec. IV). Compact analytical expressions, explicitly showing the symmetry properties of P_{ee} and useful for practical calculations, are summarized in the final section (Sec. V), to which we refer the impatient reader.

II. TWO-FLAVOR TRANSITIONS

In this section we discuss numerical and analytical calculations of the survival probability P_{ee} for neutrinos and antineutrinos, assuming two-family mixing between ν_e and another active neutrino ($\nu_a = \nu_\mu$ or ν_τ). A simple analytical prescription will be shown to reproduce very accurately the exact numerical results for P_{ee}.

---

[1] The key role of $P_{ee}(\nu)$ and $P_{ee}(\overline{\nu})$, related to the practical undistinguishability of supernova muon and tau (anti)neutrinos, is neatly discussed in [5,7].

A. 2ν transitions: Notation

In the case of two-family $\nu_e \to \nu_a$ oscillations ($a = \mu$ or τ), we label the mass (m) eigenstates (ν_1, ν_2) so that ν_1 is the lightest,

$$\Delta m^2 = m_2^2 - m_1^2 > 0 \ , \tag{1}$$

and parametrize the mixing matrix U as

$$\begin{pmatrix} U_{e1} & U_{e2} \\ U_{a1} & U_{a2} \end{pmatrix} = \begin{pmatrix} \cos\theta & \sin\theta \\ -\sin\theta & \cos\theta \end{pmatrix} \ , \tag{2}$$

where $\theta \in [0, \pi/2]$. In vacuum, $\nu_e \to \nu_a$ oscillations can be described in terms of the pathlength (x) and of the oscillation wavenumber

$$k = \Delta m^2/2E \ , \tag{3}$$

E being the neutrino energy. In matter, the $\nu_e \to \nu_a$ dynamics also depends on the $\nu_e - \nu_a$ interaction potential difference [27]

$$V(x) = \sqrt{2}\, G_F\, N_e(x) \ , \tag{4}$$

where $N_e(x)$ is the electron density profile. In appropriate units,

$$\frac{V(x)}{\mathrm{eV}^2/\mathrm{MeV}} = 7.57 \times 10^{-8}\, Y_e(x)\, \frac{\rho(x)}{\mathrm{g/cm}^3} \ , \tag{5}$$

where $\rho(x)$ is the matter density and $Y_e(x)$ is the electron/nucleon number fraction.

In supernovae, $\rho(x)$ [and thus $V(x)$] can be approximately described by a power law, $\rho(x) \propto x^{-3}$ [28]. In the present work, power-law potentials are parametrized as

$$V(x) = V_0 \left(\frac{x}{R_\odot} \right)^{-n} \ , \tag{6}$$

where $n = 3$ (unless otherwise stated), and distances are conventionally reported in units of the solar radius, $R_\odot = 6.96 \times 10^8$ m.

Figure 1 shows an example of "realistic" neutrino potential profile $V(x)$ (dashed curve), as graphically reduced from the supernova simulation published in [29] for the case of $M = 14.6\, M_\odot$, M being the mass of the ejecta. In the same figure, the solid line represents the best-fit power-law potential ($n = 3$), corresponding to take $V_0 = 1.5 \times 10^{-8}$ eV^2/MeV in Eq. (6). For definiteness, we will use the realistic or the power-law curves in Fig. 1 as representative $V(x)$ profiles for our calculations. However, our main results are applicable to generic supernova density profiles.

B. 2ν transitions: Neutrinos

Following [5], the calculation of $P_{ee}(\nu)$ from the initial ν state in matter to the final ν detection in vacuum[2] can be factorized as

$$P_{ee}(\nu) = \left(1 \, , \; 0 \right) \left(\begin{array}{cc} \cos^2\theta & \sin^2\theta \\ \sin^2\theta & \cos^2\theta \end{array} \right) \left(\begin{array}{cc} 1 - P_c(\nu) & P_c(\nu) \\ P_c(\nu) & 1 - P_c(\nu) \end{array} \right) \left(\begin{array}{cc} \cos^2\theta_m & \sin^2\theta_m \\ \sin^2\theta_m & \cos^2\theta_m \end{array} \right) \left(\begin{array}{c} 1 \\ 0 \end{array} \right) \, , \quad (7)$$

where $P_c(\nu)$ is the so-called crossing probability for neutrinos[3] [$P_c(\nu) = P(\nu_{2m} \to \nu_1)$], and θ_m is the effective mixing angle in matter at the origin, defined by

$$\sin 2\theta_m = \frac{\sin 2\theta}{\sqrt{(\cos 2\theta - V/k)^2 + \sin^2 2\theta}} \, , \quad (8)$$

$$\cos 2\theta_m = \frac{\cos 2\theta - V/k}{\sqrt{(\cos 2\theta - V/k)^2 + \sin^2 2\theta}} \, . \quad (9)$$

Note that in Eq. (7) it is understood that oscillating terms are averaged out, thus providing an incoherent ν state at detection.

The high supernova core density (at the start of neutrino free streaming) implies $V/k \gg 1$ in Eqs. (8) and (9), so that $\sin 2\theta_m \simeq 0$ and $\cos 2\theta_m \simeq -1$. From Eq. (7), one can then reduce the calculation of P_{ee} to that of P_c,

$$P_{ee}(\nu) = \cos^2\theta \, P_c(\nu) + \sin^2\theta \, [1 - P_c(\nu)] \quad (10)$$

$$= U_{e1}^2 \, P_c(\nu) + U_{e2}^2 \, [1 - P_c(\nu)] \, . \quad (11)$$

1. Numerical approach

One possible approach to the calculation of P_c (and P_{ee}) is the numerical integration of the neutrino evolution equations along the supernova potential profile, as advocated in some recent works [18–20], as well as in a few earlier ones (see, e.g., [24]). For the purposes of our work, we have performed a numerical (Runge-Kutta) calculation for P_c, assuming the two potential profiles in Fig. 1.

Figures 2 and 3 show our numerical results as dotted isolines for $P_c(\nu)$ in the mass-mixing plane ($\Delta m^2/E$, $\tan^2\theta$), for the case of power-law and realistic potential, respectively.[4] The "bumpy" structure of the realistic $V(x)$ profile is reflected by the "wiggling" behavior of P_c in Fig. 3, leading to significant differences with the P_c isolines of Fig. 2 in part of the

---

[2]The discussion of possible Earth matter effects is postponed to Sec. IV.

[3]The cases $P_c \simeq 0$ and $P_c \neq 0$ discriminate adiabatic and nonadiabatic transitions in matter.

[4]The solid curves in Figs. 2 and 3 correspond to our analytical approximation for P_c, as discussed later.

parameter space. However, one can note that, for $\Delta m^2/E \to 0$, the detailed structure of $V(x)$ is irrelevant, and $P_c(\nu) \to \cos^2\theta$ in both Figs. 2 and 3 (extremely nonadiabatic limit).

Although brute-force numerical calculations of P_c can provide, in principle, "exact" results, it should be stressed that they do not represent an optimal and efficient approach in the case of supernovae. Computer routines for integration are tipically time-consuming, being required to track a large number of oscillation cycles along a potential profile spanning many orders of magnitude. Instabilities and inaccuracies in the numerical results can easily emerge for realistic potentials (as experienced by ourselves), as a consequence of sudden variations in the lowest order $V(x)$ derivatives.[5] Moreover, numerical integration produces additional but useless (unobservable) information on oscillating factors and phases, and is thus inefficient for practical purposes.[6] Last, but not least, the uncertainties affecting simulated supernova density profiles make it preferable to perform several approximated (but quick) calculations of P_c for different trial functions $V(x)$, rather than a single (but time-consuming) exact numerical calculation for a fixed $V(x)$.

2. Analytical approach

The previous discussion indicates that a handy analytical approximation to the numerical results for P_c, applicable in the whole parameter space, is highly desirable. We propose (and motivate below) the following analytical recipe in three steps:
(*i*) Identify the point x_p where *the potential equals the wavenumber*,

$$V(x_p) = k \ ; \tag{12}$$

(*ii*) calculate the so-called *density scale factor* r at that point,

$$r = -\left[\frac{1}{V(x)}\,\frac{dV(x)}{dx}\right]^{-1}_{x=x_p} \ ; \tag{13}$$

(*iii*) Insert the above r in the *double-exponential* parametrization for $P_c(\nu)$ (originally derived in the context of solar neutrinos [25,26]),

$$P_c(\nu) = \frac{\exp(2\pi r k\cos^2\theta) - 1}{\exp(2\pi r k) - 1} \ . \tag{14}$$

The results of such an exceedingly simple analytical recipe are shown as solid isolines for P_c in Fig. 2 (power-law case) and Fig. 3 (realistic case), to be compared with the corresponding dashed isolines (exact numerical results). The agreement between numerical and

---

[5]Indeed, we think that some numerical artifacts (fake wiggles) might be present in the numerical calculations of P_{ee} as graphically reported in [24].

[6]For instance, the authors of [18,19] need to time-average their numerical probabilities, in order to force an incoherent initial state for the implementation of Earth matter effects.

analytical estimates of P_c is extremely good in the whole parameter space, the difference being $\delta P_c = 2 \times 10^{-2}$ in the worst cases.[7] The final accuracy for P_{ee} is even better, since Eq. (10) implies $\delta P_{ee} = |\cos 2\theta| \delta P_c < \delta P_c$.

Notice that, in the exact power-law case [Eq. (6)], the calculation of r through Eqs. (12) and (13) is trivial,

$$\frac{r}{R_\odot} = \frac{1}{n} \left(\frac{V_0}{k} \right)^{1/n} \quad . \tag{15}$$

In the case of realistic potential profile, the only modest complication is the numerical solution of Eq. (12) and the evaluation of the derivative in Eq. (13) for the given (tabulated or parametrized) function $V(x)$.

Our effective analytical prescription for $P_c(\nu)$ in supernovae [Eqs. (12)–(14)] stems from several recent improvements in the understanding of nonadiabatic transitions, as discussed below. Although such improvements have been mainly tested in solar neutrino oscillations, they are often applicable also to supernova ν oscillations.

3. Discussion of the analytical prescription

Equation (14), originally derived for the solar neutrino (exponential) density profile [25,26] within the unnecessary restriction $\theta < \pi/4$, was explicitly shown in [30,31] to hold for $\theta \geq \pi/4$ as well, especially for appropriately chosen density scale factors r [23]. The double-exponential form of P_c for $\theta \geq \pi/4$ has also been recently applied to the transitions of high-energy neutrinos from the decay of hypothetical massive particles trapped in the Sun [32], and to the transitions of supernova neutrinos [15–17]. Such parametrization for P_c has thus several desirable properties: (*i*) It is a good ansatz (as originally advocated in [33]) for generic density profiles; (*ii*) It holds in both octants of θ; (*iii*) It reproduces the extremely nonadiabatic limit at small k; and (*iv*) It reproduces the single-exponential, Landau-Zener (LZ) limit at small θ (see, e.g., [5]). As a final remark on Eq. (14), it should be noted that the single- and double-exponential forms for P_c involve, in general, a function $F(\theta)$ depending on the potential profile (see Table I in [33]). Our choice in Eq. (14) corresponds to take $F(\theta) = 1 - \tan^2 \theta$, which is the exact result for a solar-like (exponential) profile, and represents the leading prefactor of F in a $1/n$ expansion[8] for a supernova-like (power-law) profile [33]. We have checked that the inclusion of the full (more complicated) expression for $F(\theta)$ in the power-law case [33,5,16] does not lead to a significant improvement in the (already high) accuracy of P_c of our analytical prescription, and thus we advocate the simpler form for P_c given in Eq. (14) also for supernovae.

The concept of a "running" density scale factor $r = r(x_p)$ [as in Eq. (13)] was also originally introduced in the context of solar neutrinos [26], typically by calculating r at the

---

[7] We have investigated a variety of supernova density profiles available in the published or unpublished literature, and obtained similarly good results (not shown).

[8] The exponential profile case can be seen as the $n \to \infty$ limit of the power-law profile case [33].

point $x_p = x_{\rm res}$ defined by the so-called "resonance" condition $V(x_{\rm res}) = \Delta m^2 \cos 2\theta$ (see, e.g., [33]). Such a choice for x_p, although successful at relatively small θ, is clearly not applicable for $\theta \geq \pi/4$ [34], and fails to describe correctly nonadiabatic transitions at small k, where $P_c \neq 0$ at $\theta \sim \pi/4$ [22,23]. For large θ, the resonance condition can be misleading, if not meaningless, and it is more appropriate to characterize P_c through the point $x_{\rm MVA}$ where maximum violation of adiabaticity (MVA) is attained [22,23,16]. Indeed, in the context of solar neutrinos, the prescription $x_p = x_{\rm MVA}$ for $r(x_p)$ is more accurate and physically more consistent than $x_p = x_{\rm res}$ [23]. In the context of supernova neutrino oscillations, it has also been recently suggested that $x_{\rm MVA}$ might play an important role as well [16,17], although the authors of [16,17] *do not* use the prescription $r = r(x_{\rm MVA})$, but make an improved WKB calculation of the LZ exponent for P_c (involving a numerical integration in the complex plane). However, we have verified that the prescription $r = r(x_{\rm MVA})$ gives very accurate results for P_c in the whole mass-mixing plane for supernovae (very close to the solid isolines in Figs. 2 and 3), making it unnecessary, in practice, to resort to WKB-inspired or other relatively complicated approaches. In fact, our Eq. (12) is just a suitable approximation of the MVA condition, as we now discuss.

For a monotonic $V(x)$ profile, the MVA point is uniquely defined in terms of the flex point of $\cos 2\theta_m(x)$ [23],

$$\left(\frac{d^2 \cos 2\theta_m(x)}{dx^2} \right)_{x = x_{\rm MVA}} = 0 \; . \tag{16}$$

For a power-law profile as in Eq. (6), the above equation implies that

$$V(x_{\rm MVA}) = k \cdot g(n, \theta) \; , \tag{17}$$

where

$$g(n,\theta) = \frac{\cos 2\theta}{2} \, \frac{2-n}{1-2n} \pm \sqrt{1 - \frac{2-n}{1-2n} + \left(\frac{\cos 2\theta}{2} \, \frac{2-n}{1-2n} \right)^2} \; , \tag{18}$$

and the $\pm$ sign must be chosen so that $g > 0$. For n close to 3 (supernova case), by keeping only the leading term in the expansion of the square root in $g(n,\theta)$, one obtains:

$$n = 2 \longrightarrow g = 1 \; , \tag{19}$$

$$n = 3 \longrightarrow g \simeq 1 + \frac{\cos 2\theta - 1}{10} \; , \tag{20}$$

$$n = 4 \longrightarrow g \simeq 1 + \frac{\cos 2\theta - 1}{7} \; , \tag{21}$$

namely, $g \simeq 1$ for $n \simeq 3 \pm 1$, up to $\sim 10\%$ errors.

A fractional error δ in the evaluation of $V(x_{\rm MVA})$ leads, for power-law potentials, to a fractional error δ/n in the evaluation of $r(x_{\rm MVA})$. Therefore, by setting in any case $g = 1$ [and thus $V = k$, as in Eq. (12), rather than $V = kg$, as in Eq. (17)] we expect a mere few % variation in the running value of r, which is of little relevance when r is inserted in P_c through Eq. (14), as we have numerically checked.

In conclusion, the condition $V(x_p) = k$ in Eq. (12) represents a good approximation to the MVA condition for supernova neutrino oscillations, and can be used to replace the time-honored (but inapplicable at large θ) resonance prescription.[9] One has then to calculate [through Eq. (13)] the corresponding (running) value of the density scale factor $r = r(x_p)$ [provided by Eq. (15) for an exact power-law profile], insert r in the double-exponential form for P_c [Eq. (14)], and finally get P_{ee} through Eq. (10). Our analytical prescription is applicable to generic (power-law or realistic) $V(x)$ profiles in the whole 2ν parameter space, with a typical percent accuracy in P_{ee}.

Figure 4 explicitly reports the results of such a prescription for P_{ee} for the two profiles in Fig. 1, and for a representative supernova ν energy ($E = 15$ MeV). Notice that the P_{ee} isolines for the power-law profile (dotted curves) are simply calculated through elementary functions [Eqs. (12)–(15)]. Notice also that the P_{ee} isolines for the realistic and power-law cases in Fig. 4 appear to differ significantly in two regions: (*i*) at relatively small mixing ($\tan^2\theta \lesssim 0.1$); and (*ii*) at nearly maximal mixing ($\tan^2\theta \lesssim 1$) with $\Delta m^2 \sim 10^{-8\pm1}$ eV^2. In connection with solar neutrinos, this fact implies that the detailed supernova density profile can be relevant for the oscillation parameters corresponding to the so-called small mixing angle (SMA), low Δm^2 (LOW), and quasivacuum oscillation (QVO) solutions to the solar neutrino problem [36]. Conversely, for oscillation parameters within the so-called large mixing angle (LMA) solution at $\Delta m^2 \gtrsim 10^{-5}$ eV^2, or within the multiple vacuum oscillation (VO) solutions at $\Delta m^2 \lesssim 10^{-9}$ eV^2 [36], transitions in supernova matter become, respectively, purely adiabatic or extremely nonadiabatic, with no significant dependence on the details of the $V(x)$ profile.

A final technical remark is in order. For solar neutrinos, it was shown in [23] that the MVA-inspired recipe for P_c [$r = r(x_{\rm MVA})$] has to be matched and replaced, at small k, with $r = const$ [31,22]. The constant (limiting) value for r can be elegantly derived, through a perturbative approach [23], in terms of an integral involving $V(x)$ in the convective zone of the Sun, where $V(x)$ experiences a sudden drop. Conversely, in supernovae, $V(x)$ vanishes in a smoother way at large x, and the small-k correction ($r = const$) becomes unnecessary in practice. We have numerically checked that such correction does not appreciably improve the accuracy of the simple MVA-inspired recipe in Eqs. (12)–(14). Therefore, concerning the calculation of P_c in supernova neutrino transitions, we advocate the use of Eqs. (12)–(14) in the whole 2ν parameter space.

C. 2ν transitions: Antineutrinos

The extension of our analytical prescription from the neutrino case to the antineutrino case can be obtained through the replacement $V/k \to -V/k$ in P_{ee}. By conventionally keeping $V > 0$ (and θ unaltered), this implies

---

[9] It is curious to note that, in the context of solar neutrinos, the relevance of the point where $V = k$ (as opposed to the resonance point) was suggested in [35] and then abandoned in the literature. See also [22] for an updated discussion.

$$P_{ee}(\overline{\nu}|+\Delta m^2) \equiv P_{ee}(\nu|-\Delta m^2) \ . \tag{22}$$

The change of sign of Δm^2 for neutrinos is equivalent to a swap of the mass labels $1 \leftrightarrow 2$,

$$P_{ee}(\nu|-\Delta m^2) \equiv P_{ee}(\nu|+\Delta m^2)_{1\leftrightarrow 2} \ , \tag{23}$$

corresponding to $U^2_{e1} \leftrightarrow U^2_{e2}$ and $\sin^2\theta \leftrightarrow \cos^2\theta$.[10]

The above two equations imply that, for fixed $\Delta m^2 > 0$ [Eq. (1)], $P_{ee}(\overline{\nu})$ can be obtained from Eqs. (10) and (14) through a $1 \leftrightarrow 2$ swap, namely,

$$\begin{aligned} P_{ee}(\overline{\nu}) &\equiv P_{ee}(\nu)_{1\leftrightarrow 2} \\ &= \sin^2\theta\, P_c(\overline{\nu}) + \cos^2\theta\, [1 - P_c(\overline{\nu})] \ , \end{aligned} \tag{24}$$

where

$$\begin{aligned} P_c(\overline{\nu}) &\equiv P_c(\nu)_{1\leftrightarrow 2} \\ &= \frac{\exp(2\pi r k \sin^2\theta) - 1}{\exp(2\pi r k) - 1} \ , \end{aligned} \tag{25}$$

with r [Eq. (13)] to be evaluated at the same (θ-independent) point x_p defined for the neutrino case in Eq. (12). Isolines of $P_c(\overline{\nu})$ from Eq. (25) are just the mirror images (around the axis $\tan^2\theta = 1$) of those obtained for $P_c(\nu)$ in Figs. 2 and 3.

D. 2ν transitions: Summary

A neat summary of the previous analytical results for ν and $\overline{\nu}$ can be obtained by introducing a new notation,

$$P_c^{\pm} \equiv \frac{\exp(\pm 2\pi r k \cos^2\theta) - 1}{\exp(\pm 2\pi r k) - 1} \tag{26}$$

$$= \begin{cases} P_c(\nu) & (+) \ , \\ 1 - P_c(\overline{\nu}) & (-) \ . \end{cases} \tag{27}$$

In terms of $P_c^{\pm}$, the expressions of $P_{ee}(\nu)$ and $P_{ee}(\overline{\nu})$ for 2ν transitions are unified as

$$P^{2\nu}_{ee} = U^2_{e1}\, P_c^{\pm} + U^2_{e2}\, (1 - P_c^{\pm}) \ , \tag{28}$$

where the $+$ sign applies to neutrinos, while the $-$ sign to antineutrinos.

In the above equation, for any sign ($\pm$), both V and k are kept > 0. All physical cases are covered by letting θ span its whole range $[0, \pi/2]$. The density scale factor r [Eq. (13)] is calculated at the point x_p where $V(x_p) = k$ [Eq. (12)]. The accuracy of such analytical prescription, as compared with exact numerical results, is at the percent level for both realistic and power-law density profiles, as demonstrated in Figs. 2 and 3 for the representative cases shown in Fig. 1. In the power-law case [Eq. (6)], the calculation of r is further simplified [Eq. (15)].

---

[10] Such well-known 2ν symmetry properties are repeated here, in preparation of the more complicated 3ν case.

III. THREE-FLAVOR TRANSITIONS WITH HIERARCHICAL MASS SPECTRA

Supernova neutrinos can provide peculiar tests of three-flavor oscillations in matter, owing to the wide dynamical range of $V(x)$ in collapsing stars (see [7–14,18–20] and references therein for recent 3ν studies). It is thus important to generalize the previous 2ν results to the case of 3ν transitions, as we do in this section for the phenomenologically interesting cases with hierarchical mass spectra. We think it useful to review the derivation of $P_{ee}^{3\nu}$ (recovering some known results) with no reference to the often (mis)used concept of "resonant transition."

A. 3ν transitions: Notation and phenomenological input

We assume mixing among three active neutrinos (ν_e, ν_μ, ν_τ) and three mass eigenstates (ν_1, ν_2, ν_3) through a unitary matrix[11] U. The matrix elements U_{ei} relevant for $P_{ee}^{3\nu}$ are parametrized in terms of two mixing angles $(\phi, \omega) = (\theta_{13}, \theta_{12})$ [5],

$$U_{e1}^2 = \cos^2\phi \, \cos^2\omega \; , \tag{29}$$

$$U_{e2}^2 = \cos^2\phi \, \sin^2\omega \; , \tag{30}$$

$$U_{e3}^2 = \sin^2\phi \; . \tag{31}$$

The kinematical parameters are completed by two independent squared mass differences $(\delta m^2, m^2)$. The dynamics is fixed by $V(x)$, and the full supernova 3ν parameter space $S_{3\nu}$ is

$$S_{3\nu} = (\delta m^2, m^2, \omega, \phi, V) \; . \tag{32}$$

Solar and reactor neutrino oscillation analyses suggest [36,37]

$$\delta m^2 = |m_2^2 - m_1^2| \lesssim 7 \times 10^{-4} \; \mathrm{eV}^2 \; , \tag{33}$$

while atmospheric neutrino analyses indicate [37,38]

$$m^2 \simeq |m_3^2 - m_{1,2}^2| \sim 3 \times 10^{-3} \; \mathrm{eV}^2 \; , \tag{34}$$

thus favoring the so-called hierarchical hypothesis [39]

$$\delta m^2 \ll m^2 \; , \tag{35}$$

very often used in the literature.

Under the assumption of Eq. (35), we parametrize the mass spectra (up to an overall mass scale) as

[11] In the context of supernova neutrinos, U can be taken real without loss of generality.

$$(m_1^2, m_2^2, m_3^2) = \begin{cases} \left(-\frac{\delta m^2}{2},\, +\frac{\delta m^2}{2},\, +m^2\right) \ , & \text{direct hierarchy} \ , \\ \left(-\frac{\delta m^2}{2},\, +\frac{\delta m^2}{2},\, -m^2\right) \ , & \text{inverse hierarchy} \ , \end{cases} \tag{36}$$

where, conventionally, $m_3^2 - m_{1,2}^2 > 0$ (< 0) identifies the so-called case of direct (inverse) hierarchy, while $m_2^2 - m_1^2 > 0$ for both hierarchies. As far as $\phi, \omega \in [0,\, \pi/2]$, such a convention can be shown to cover all physical cases, both in vacuum and in matter [40].

Besides Eqs. (33)–(35), a further phenomenological input comes from the combination of reactor and atmospheric neutrino data, providing [37,38]

$$\sin^2 \phi = U_{e3}^2 \lesssim \text{few } \% \ . \tag{37}$$

As a consequence of the hierarchical assumption of Eq. (35) [and, to some extent, also of Eq. (37)], the 3ν dynamics approximately reduces to the dynamics in two 2ν subsystems, dominated by relatively low (L) and high (H) values of the matter density, according to parameter space factorization

$$S_{3\nu} \simeq L_{2\nu} \otimes H_{2\nu} \ = (\delta m^2,\, \omega,\, V \cos^2 \phi) \otimes (m^2,\, \phi,\, V) \tag{38}$$

(see [5] and references therein). The corresponding "low" and "high" neutrino oscillation wavenumbers are defined by

$$k_L = \delta m^2 / 2E \tag{39}$$

and

$$k_H = m^2 / 2E \ , \tag{40}$$

respectively.

B. 3ν transitions: Neutrinos with direct hierarchy

For neutrinos with direct mass hierarchy, the factorization of dynamics in Eq. (38) leads to [5]

$$\begin{aligned} P_{ee}(\nu) = \left(U_{e1}^2 \,,\ U_{e2}^2 \,,\ U_{e3}^2 \right) & \begin{pmatrix} 1 - P_L(\nu) & P_L(\nu) & 0 \\ P_L(\nu) & 1 - P_L(\nu) & 0 \\ 0 & 0 & 1 \end{pmatrix} \\ \times & \begin{pmatrix} 1 & 0 & 0 \\ 0 & 1 - P_H(\nu) & P_H(\nu) \\ 0 & P_H(\nu) & 1 - P_H(\nu) \end{pmatrix} \begin{pmatrix} U_{e1,m}^2 \\ U_{e2,m}^2 \\ U_{e3,m}^2 \end{pmatrix} \ , \end{aligned} \tag{41}$$

where P_L and P_H are the crossing probabilities for the low and high density transitions, respectively, and the elements $U_{ei,m}^2$ in matter are defined in analogy to Eqs. (29)–(31), but with neutrino mixing angles ω_m and ϕ_m in matter given by

$$\sin 2\omega_m = \frac{\sin 2\omega}{\sqrt{(\cos 2\omega - \cos^2\phi\, V/k_L)^2 + \sin^2 2\omega}} \; , \tag{42}$$

$$\cos 2\omega_m = \frac{\cos 2\omega - V/k_L}{\sqrt{(\cos 2\omega - \cos^2\phi\, V/k_L)^2 + \sin^2 2\omega}} \; , \tag{43}$$

and

$$\sin 2\phi_m = \frac{\sin 2\phi}{\sqrt{(\cos 2\omega - V/k_H)^2 + \sin^2 2\phi}} \; , \tag{44}$$

$$\cos 2\phi_m = \frac{\cos 2\phi - V/k_H}{\sqrt{(\cos 2\omega - V/k_H)^2 + \sin^2 2\phi}} \; , \tag{45}$$

at zeroth order in $\delta m^2/m^2$ [5]. The (high density) initial condition $V/k_{L,H} \gg 1$ leads then to $\cos 2\phi_m \simeq -1 \simeq \cos 2\omega_m$ and to the known expression

$$P_{ee}(\nu) = U_{e1}^2\, P_L(\nu)\, P_H(\nu) + U_{e2}^2\, [1 - P_L(\nu)]\, P_H(\nu) + U_{e3}^2\, [1 - P_H(\nu)] \; . \tag{46}$$

On the basis of Eq. (38) and of our 2ν prescription in Eqs. (12)–(14), $P_L(\nu)$ and $P_H(\nu)$ can be analytically expressed as

$$P_L(\nu) = \frac{\exp(2\pi r_L k_L \cos^2\omega) - 1}{\exp(2\pi r_L k_L) - 1} \tag{47}$$

and

$$P_H(\nu) = \frac{\exp(2\pi r_H k_H \cos^2\phi) - 1}{\exp(2\pi r_H k_H) - 1} \; , \tag{48}$$

where

$$r_{L,H} = - \left[\frac{1}{V(x)} \, \frac{dV(x)}{dx} \right]^{-1}_{x = x_{L,H}} \; , \tag{49}$$

and the points x_L and x_H are defined by the $V = k$ condition[12] [Eq. (12)]

$$V(x_{L,H}) = k_{L,H} \; . \tag{50}$$

Equations (46)–(50) allow the calculation of $P_{ee}(\nu)$ in the whole 3ν parameter space for direct hierarchy.

---

[12]In principle, Eq. (38) implies an effective potential $V(x)\cos^2\phi$ for the L subsystem, and thus $V(x_L)\cos^2\phi = k_L$. However, we have checked that, within the phenomenological bound in Eq. (37), the resulting difference in the calculation of P_{ee} is completely negligible. We prefer then the simpler condition $V(x_L) = k_L$, analogous to $V(x_H) = k_H$ for the H subsystem.

C. 3ν transitions: Antineutrinos with direct hierarchy

The antineutrino case can be obtained in analogy to the neutrino case [Eqs. (41)–(45)] through the replacement $V/k_{L,H} \to -V/k_{L,H}$. In particular, the *antineutrino* mixing angles in matter are given by

$$\sin 2\overline{\omega}_m = \frac{\sin 2\omega}{\sqrt{(\cos 2\omega + V\cos^2\phi/k_L)^2 + \sin^2 2\omega}} \; , \tag{51}$$

$$\cos 2\overline{\omega}_m = \frac{\cos 2\omega + V/k_L}{\sqrt{(\cos 2\omega + V\cos^2\phi/k_L)^2 + \sin^2 2\omega}} \; , \tag{52}$$

and analogously for $\overline{\phi}_m$. The initial high-density condition gives $\cos 2\overline{\phi}_m \simeq +1 \simeq \cos 2\overline{\omega}_m$ and leads to

$$P_{ee}(\overline{\nu}) = U_{e1}^2\,[1 - P_L(\overline{\nu})] + U_{e2}^2\,P_L(\overline{\nu}) \; . \tag{53}$$

Our analytical prescription for $P_L(\overline{\nu})$ is then obtained, *mutatis mutandis*, from Eq. (25),

$$P_L(\overline{\nu}) = \frac{\exp(2\pi r_L k_L \sin^2\omega) - 1}{\exp(2\pi r_L k_L) - 1} \; , \tag{54}$$

with r_L defined as in Eqs. (49) and (50).

D. 3ν transitions: Neutrinos with inverse hierarchy

For fixed mass spectrum and mixing angles, neutrino and antineutrino probabilities can be transformed one into the other by flipping the signs of $V/k_{L,H}$ or, equivalently, by flipping the signs attached to δm^2 and m^2, while keeping $V > 0$. The $\pm\delta m^2$ sign flip is equivalent to the $1 \leftrightarrow 2$ swap of mass labels (as discussed for the 2ν case), leading to $U_{e1}^2 \leftrightarrow U_{e2}^2$ [namely, $\sin^2\omega \leftrightarrow \cos^2\omega$, with no change in ϕ or U_{e3}^2]. The $\pm m^2$ sign flip is instead equivalent to swap hierarchy [see Eq. (36)].

From such symmetry properties one obtains

$$P_{ee}(\nu\,|\,+\delta m^2,\,-m^2) \equiv P_{ee}(\overline{\nu}|\,-\delta m^2,\,+m^2) \equiv P_{ee}(\overline{\nu}\,|\,+\delta m^2,\,+m^2)_{1\leftrightarrow 2} \; , \tag{55}$$

namely, the ν_e survival probability for inverse hierarchy equals the $\overline{\nu}_e$ survival probability for direct hierarchy [Eq. (53)], under the substitution $U_{e1}^2 \leftrightarrow U_{e2}^2$,

$$P_{ee}(\nu) = U_{e2}^2\,[1 - P_L(\nu)] + U_{e1}^2\,P_L(\nu) \; , \tag{56}$$

with $P_L(\nu)$ defined as in Eq. (47).

E. 3ν transitions: Antineutrinos with inverse hierarchy

In analogy with the previous subsection, it can be easily realized that

$$P_{ee}(\overline{\nu}\,|+\delta m^2,\,-m^2) \equiv P_{ee}(\nu|-\delta m^2,\,+m^2) \equiv P_{ee}(\nu\,|+\delta m^2,\,+m^2)_{1\leftrightarrow 2}\ , \tag{57}$$

which, applied to Eq. (46), gives

$$P_{ee}(\overline{\nu}) = U_{e2}^2\,P_L(\overline{\nu})\,P_H(\nu) + U_{e1}^2\,[1-P_L(\overline{\nu})]\,P_H(\nu) + U_{e3}^2\,[1-P_H(\nu)]\ , \tag{58}$$

with $P_L(\overline{\nu})$ and $P_H(\nu)$ defined as in Eqs (54) and (48), respectively.

Notice that we have written $P_H(\nu)$ and not $P_H(\overline{\nu})$ in Eq. (58), since the $1 \leftrightarrow 2$ swap makes no change in P_H, defined in terms of $m_3^2 - m_{1,2}^2$ and of U_{e3}^2. One can then drop the argument of P_H and simply write[13]

$$P_H(\overline{\nu}) = P_H(\nu) \equiv P_H\ . \tag{59}$$

F. 3ν transitions: Summary I

The 3ν results in Eqs. (46), (53), (56), and (58) can be summarized as

$$P_{ee}^{3\nu} = U_{e1}^2 X_1 + U_{e2}^2 X_2 + U_{e3}^2 X_3\ , \tag{60}$$

where the coefficients X_i are given in Table I, in terms of $P_L(\nu)$, $P_L(\overline{\nu})$, and P_H.

The parametrization of $P_{ee}^{3\nu}$ given in Eq. (60) and Table I agrees with the results previously obtained in [7,9]. In addition, however, we have provided explicit analytical approximations for P_L [Eqs. (47) and (54)] and for P_H [Eq. (48)], allowing a straightforward calculation of $P_{ee}^{3\nu}$ in the whole mass-mixing parameter space, for generic (realistic or power-law) potential profiles.

G. 3ν transitions: Summary II

An alternative summary for $P_{ee}^{3\nu}$ can be obtained by introducing, in analogy with the 2ν case, the notation

$$P_L^{\pm} = \frac{\exp(\pm 2\pi r_L k_L \cos^2\omega) - 1}{\exp(\pm 2\pi r_L k_L) - 1} \tag{61}$$

$$= \begin{cases} P_L(\nu) & (+)\ , \\ 1 - P_L(\overline{\nu}) & (-)\ , \end{cases} \tag{62}$$

---

[13] A formal distinction between $P_H(\nu)$ and $P_H(\overline{\nu})$ was kept in the notation of [7] and then dropped in [9].

and

$$P_H^{\pm} = \frac{\exp(\pm 2\pi r_H k_H \cos^2\phi) - 1}{\exp(\pm 2\pi r_H k_H) - 1} \tag{63}$$

$$\simeq \begin{cases} \exp(-2\pi r_H k_H \sin^2\phi) & (+) \ , \\ 1 & (-) \ , \end{cases} \tag{64}$$

where, in the last equation, we have used the phenomenological inputs in Eqs. (34) and (37), implying that $2\pi r_H k_H \cos^2\phi \gg 1$ for typical supernova potential profiles and neutrino energies.

Equation (60) can then be written in the equivalent form

$$P_{ee}^{3\nu} = U_{e1}^2 \, P_L^{\pm} \, P_H^{\pm} + U_{e2}^2 \, (1 - P_L^{\pm}) \, P_H^{\pm} + U_{e3}^2 \, (1 - P_H^{\pm}) \ , \tag{65}$$

where the sign assignment for $P_{L,H}^{\pm}$ is given in Table II for the four possible combinations of neutrino types (ν or $\overline{\nu}$) and mass hierarchy (direct or inverse).

The neat 3ν summary given in Eqs. (61), (63), (65) and in Table II makes the symmetry properties of $P_{ee}^{3\nu}$ rather transparent. Passing from ν to $\overline{\nu}$, or from direct to inverse hierarchy, appears to simply require appropriate sign flips.

H. 3ν transitions: Representative P_{ee} calculations

Figure 5 shows a representative analytical calculation of $P_{ee}^{3\nu}$ in the slice $(\delta m^2, \tan^2\omega)$ of the 3ν parameter space, which is relevant for the L transition in supernovae [Eq. (38)] and for its connection with solar neutrino oscillations. Calculations (solid lines)[14] are made at fixed $E = 15$ MeV, $m^2 = 3 \times 10^{-3}$ eV^2, and $\tan^2\phi = 4 \times 10^{-5}$ ($P_H^+ = 0.48$), for the power-law profile in Fig. 1. The upper panels refer to ν (left) and $\overline{\nu}$ (right) in the case of direct hierarchy. The lower panels refer to ν (left) and $\overline{\nu}$ (right) in the case of inverse hierarchy. Notice that all calculations for this figure involve only elementary functions, the density scale factor r being explicitly given by Eq. (15) for a power-law profile.

A glance at Fig. 5 shows two apparent symmetries: $P_{ee}(\nu)$ and $P_{ee}(\overline{\nu})$ for direct hierarchy look like the mirror image of $P_{ee}(\overline{\nu})$ and $P_{ee}(\nu)$ for inverse hierarchy, respectively. This (approximate) symmetry originates from the small value of U_{e3}^2 used in the calculations of Fig. 5. Indeed, neglecting the third term (proportional to U_{e3}^2) in Eq. (65), and using Eq. (28) (with the identification $P_c^{\pm} = P_L^{\pm}$), it is

$$P_{ee}^{3\nu} \simeq P_H^{\pm} \, P_{ee}^{2\nu} \ , \tag{66}$$

namely, the 3ν probability is obtained from the 2ν probability through a modulation factor $P_H^{\pm}$. Using Eq. (66) and the symmetry properties in Eqs. (55) and (57), it follows that

$$P_{ee}^{3\nu}(\nu, \text{ direct}) \simeq P_H^{+} \, P_{ee}^{2\nu}(\nu) = P_H^{+} \, P_{ee}^{2\nu}(\overline{\nu})_{1 \leftrightarrow 2} \simeq P_{ee}^{3\nu}(\overline{\nu}, \text{ inverse})_{1 \leftrightarrow 2} \tag{67}$$

---

[14] The dotted curves in Fig. 5 include Earth matter effects, to be discussed in the next Section.

and

$$P^{3\nu}_{ee}(\overline{\nu},\,\text{direct}) \simeq P^{-}_{H}\, P^{2\nu}_{ee}(\overline{\nu}) = P^{-}_{H}\, P^{2\nu}_{ee}(\nu)_{1\leftrightarrow 2} \simeq P^{3\nu}_{ee}(\nu,\,\text{inverse})_{1\leftrightarrow 2}\ , \tag{68}$$

as previously observed in Fig. 5. We remark that the above Eqs. (67) and (68) represent approximate mirror symmetries, which become exact only for $U^2_{e3} = 0$. However, for U^2_{e3} obeying the bound in Eq. (37), such symmetries are broken, at most, at the few percent level.

IV. INCLUDING EARTH MATTER EFFECTS

We briefly review known analytical results about Earth matter effects, for the sake of completeness and self-consistency of the paper. For recent phenomenological studies of such effects in the supernova neutrino context see, e.g., [7–9,18–20].

In general, possible Earth matter effects preceding supernova ν detection can be implemented by the final-state substitution [5]

$$(U^2_{e1},\, U^2_{e2},\, U^2_{e3}) \to (P_{e1},\, P_{e2},\, P_{e3}) \tag{69}$$

in Eq. (60) or (65), where $P_{ei} = P(\nu_e \to \nu_i)$ in the Earth.

Under the assumption of mass spectrum hierarchy (either direct or inverse), the 3ν calculation of P_{ei} is further reduced to a 2ν problem [7],

$$(P_{e1},\, P_{e2},\, P_{e3}) \simeq [\cos^2\phi\,(1-P_E),\, \cos^2\phi\, P_E,\, \sin^2\phi]\ , \tag{70}$$

where

$$P_E = P^{2\nu}_{e2}\,. \tag{71}$$

The task is thus reduced to the 2ν calculations of $P_E(\nu)$ and $P_E(\overline{\nu})$, which are independent on $\pm m^2$ and on the hierarchy type (direct or inverse). Analytical expressions for P_E can be given for particularly simple (or approximated) situations of Earth matter crossing.

A. One shell

If the ν trajectory crosses only the Earth mantle, characterized by an approximately constant (average) density, $P_E(\nu)$ is simply given by

$$P_E(\nu) = \sin^2\omega + \sin 2\omega_m\, \sin(2\omega_m - 2\omega)\, \sin^2\left(\frac{k_L\, \sin 2\omega}{2\, \sin 2\omega_m}\, L\right) \tag{72}$$

where L is the total pathlength in the mantle, and ω_m is defined as in Eqs. (42) and (43) with the appropriate potential V in the mantle [Eqs. (4) and (5)]. The antineutrino probability is obtained through the substitution

$$P_E(\overline{\nu}) = P_E(\nu)\Big|_{V/k_L \to\, -V/k_L}\ , \tag{73}$$

leading to

$$P_E(\overline{\nu}) = \sin^2\omega + \sin 2\overline{\omega}_m \, \sin(2\overline{\omega}_m - 2\omega) \, \sin^2\left(\frac{k_L \, \sin 2\omega}{2 \, \sin 2\overline{\omega}_m} \, L\right) \, , \tag{74}$$

where $\overline{\omega}_m$ is defined through Eqs. (51) and (52).

Figure 5 shows an example of Earth matter effects on $P_{ee}^{3\nu}$ for mantle crossing (dotted curves), assuming $\rho = 4.5$ g/cm^3, $Y_e = 0.5$, and $L = 8500$ km (parameters which are of interest for SN1987A phenomenology; see, e.g., [8,9]). The neutrino potential in the mantle is then $V_M = 1.7 \times 10^{-7}$ eV^2/MeV, implying strong effects for $V_M \sim k_L$ and thus for $\delta m^2 \sim 2EV \sim O(10^{-6})$ eV^2, which may be relevant in connection with the so-called LMA solution to the solar neutrino problem [36], as widely discussed recently [7–9,18–20]. Notice that the approximate symmetries in Eqs. (67) and (68) are preserved by Earth matter effects, since they act mainly on the two-neutrino L transition in hierarchical approximation [Eq. (70)].

B. Multiple shells

Neutrino oscillations across two Earth shells with different densities [mantle (M) + core (C)] were considered in [41] in the context of supernovae, and intensively studied in [42,43] on general grounds, with emphasis on interesting interference properties peculiar to layered matter (see also [44]). Adapting, e.g., the notation of [43] to ours, the expression of $P_E(\nu)$ for a mantle+core+mantle path in the Earth ($L = L_M + L_C + L_M$) reads

$$P_E(\nu) = \sin^2\omega + W_1 \, (W_1 \, \cos 2\omega + W_3 \, \sin 2\omega) \, , \tag{75}$$

where $W_{1,3}$ are the first and third component of the vector

$$\mathbf{W} = 2 \, S_M \, Y \, \mathbf{n}_M + S_C \, \mathbf{n}_C \, , \tag{76}$$

having defined Y as

$$Y = C_M \, C_C - (\mathbf{n}_M \cdot \mathbf{n}_C) \, S_M \, S_C \, , \tag{77}$$

the vectors $\mathbf{n}_M$ and $\mathbf{n}_C$ as

$$\mathbf{n}_{M,C} = (\sin 2\omega_{M,C}, \, 0, \, -\cos 2\omega_{M,C}) \, , \tag{78}$$

and C_M and C_C as

$$C_{M,C} = \cos\left(\frac{k_L \, \sin 2\omega}{2 \, \sin 2\omega_{M,C}} \, L_{M,C}\right) \tag{79}$$

(and similarly for $S_{M,C}$, with $\cos \to \sin$), where ω_M and ω_C are the effective neutrino mixing angles in the mantle and in the core. $P_E(\overline{\nu})$ is then obtained from $P_E(\nu)$ through the replacement indicated in Eq. (73).

In the general case of N different shells, not necessarily with constant density in each shell, the calculation of P_E can also be performed analytically, through the perturbative approach developed in [45] in the context of solar neutrinos.

V. SUMMARY AND CONCLUSIONS

In the context of two-flavor (anti)neutrino transitions in supernovae, we have described a simple and accurate analytical prescription for the calculation of the survival probability P_{ee}, based on a double exponential form for the crossing probability, and inspired by the condition of maximum violation of adiabaticity. The prescription holds in the whole oscillation parameter space and for generic supernova density profiles. The analytical approach has then been generalized to cover three-flavor transitions with mass spectrum hierarchy (either direct or inverse), and to include Earth matter effects.

The final prescription for $P_{ee}^{3\nu}$ can be summarized as follows:

1. Assume a supernova potential profile $V(x) > 0$;

2. Fix the mixing angles $\phi = \theta_{13}$ [obeying Eq. (37)] and $\omega = \theta_{12}$, and calculate the matrix elements U_{ei}^2 through Eqs. (29)–(30);

3. Fix the "solar" and "atmospheric" squared mass differences, $\delta m^2 > 0$ and $m^2 > 0$, respectively [within the phenomenological restrictions in Eqs. (33)–(35)];

4. At a given (anti)neutrino energy E, find the points x_L and x_H where the potential V equals the wavenumbers $k_L = \delta m^2/2E$ and $k_H = m^2/2E$, respectively:

$$V(x_{L,H}) = k_{L,H} \; ;$$

5. Calculate the corresponding density scale factors r_L and r_H as

$$r_{L,H} = - \left[\frac{1}{V(x)} \, \frac{dV(x)}{dx} \right]^{-1}_{x = x_{L,H}}$$

(both > 0 for monotonically decreasing V);

6. Assign the $\pm$ signs in $P_L^{\pm}$ and $P_H^{\pm}$ by choosing the neutrino type (ν or $\overline{\nu}$) and hierarchy (direct or inverse) in Table II, and calculate then $P_{L,H}^{\pm}$ through

$$P_L^{\pm} = \frac{\exp(\pm 2\pi r_L k_L \cos^2\omega) - 1}{\exp(\pm 2\pi r_L k_L) - 1}$$

and

$$P_H^{\pm} = \frac{\exp(\pm 2\pi r_H k_H \cos^2\phi) - 1}{\exp(\pm 2\pi r_H k_H) - 1} \; ;$$

7. Calculate $P_{ee}^{3\nu}$ as

$$P_{ee}^{3\nu} = U_{e1}^2 \, P_L^{\pm} \, P_H^{\pm} + U_{e2}^2 \, (1 - P_L^{\pm}) \, P_H^{\pm} + U_{e3}^2 \, (1 - P_H^{\pm}) \; ;$$

8. Finally, include possible Earth matter effects as reviewed in Sec. IV.

We think that such analytical prescription may be useful to simplify the calculation (and to help the understanding) of supernova neutrino oscillation effects.

ACKNOWLEDGMENTS

E.L. thanks G. Raffelt and H. Minakata for useful discussions on supernova neutrinos during the TAUP 2001 Conference. This work was supported in part by the Italian *Istituto Nazionale di Fisica Nucleare* (INFN) and *Ministero dell'Istruzione, dell'Università e della Ricerca* (MIUR) under the project "Fisica Astroparticellare."

TABLES

TABLE I. Coefficients X_i to be used in the parametrization of $P_{ee}^{3\nu}$ given in Eq. (60), according to the four possible combinations of neutrino types (ν or $\overline{\nu}$) and mass spectrum hierarchy (direct or inverse). The coefficients agree with those derived in Refs. [7,9].

Type	Hierarchy	X_1	X_2	X_3
ν	direct	$P_L(\nu)\,P_H$	$[1-P_L(\nu)]\,P_H$	$1-P_H$
$\overline{\nu}$	direct	$1-P_L(\overline{\nu})$	$P_L(\overline{\nu})$	0
ν	inverse	$P_L(\nu)$	$1-P_L(\nu)$	0
$\overline{\nu}$	inverse	$[1-P_L(\overline{\nu})]\,P_H$	$P_L(\overline{\nu})\,P_H$	$1-P_H$

TABLE II. Signs assigned to $P_L^{\pm}$ and $P_H^{\pm}$, to be used in the parametrization of $P_{ee}^{3\nu}$ given in Eq. (65), according to the four possible combinations of neutrino types (ν or $\overline{\nu}$) and mass spectrum hierarchy (direct or inverse).

Type	Hierarchy	$P_L^{\pm}$	$P_H^{\pm}$
ν	direct	$+$	$+$
$\overline{\nu}$	direct	$-$	$-$
ν	inverse	$+$	$-$
$\overline{\nu}$	inverse	$-$	$+$

REFERENCES

[1] G. Raffelt, *Stars as laboratories for fundamental physics: The astrophysics of neutrinos, axions, and other weakly interacting particles* (Chicago U. Press, Chicago, USA, 1996).

[2] P. Vogel, lecture at the Erice School on "Neutrinos in Astro, Particle, and Nuclear Physics" (Erice, Italy, 2001), nucl-th/0111016.

[3] T.J. Loredo and D.Q. Lamb, astro-ph/0107260.

[4] T.K. Kuo and J. Pantaleone, Phys. Rev. D **37**, 298 (1988).

[5] T.K. Kuo and J. Pantaleone, Rev. Mod. Phys. 61, 937 (1989).

[6] H. Nunokawa, in the Proceedings of the EURESCO Conference on Frontiers in Particle Astrophysics and Cosmology (San Feliu de Guixols, Spain, 2000), edited by M. Hirsch, G. Raffelt, and J.W.F. Valle, Nucl. Phys. B (Proc. Suppl.) **95**, 193 (2001).

[7] A.S. Dighe and A.Yu. Smirnov, Phys. Rev. D **62**, 033007 (2000).

[8] C. Lunardini and A.Yu. Smirnov, Phys. Rev. D **63**, 073009 (2001).

[9] C. Lunardini and A.Yu. Smirnov, Nucl. Phys. B **616**, 307 (2001).

[10] H. Minakata and H. Nunokawa, Phys. Lett. B **504**, 301 (2001).

[11] G. Dutta, D. Indumati, M.V.N. Murthy, and G. Rajasekaran, Phys. Rev. D **61**, 013009 (2001).

[12] G. Dutta, D. Indumati, M.V.N. Murthy, and G. Rajasekaran, Phys. Rev. D **62**, 093014 (2001).

[13] G. Dutta, D. Indumati, M.V.N. Murthy, and G. Rajasekaran, Phys. Rev. D **64**, 073011 (2001).

[14] S. Chiu and T.K. Kuo, Phys. Rev. D **61**, 073015 (2000).

[15] M. Kachelriess, R. Tomas, and J.W.F. Valle, J. of High Energy Phys. **101**, 30 (2001).

[16] M. Kachelriess and R. Tomas, Phys. Rev. D **64**, 073002 (2001).

[17] M. Kachelriess, A. Strumia, R. Tomas, and J.W.F. Valle, hep-ph/0108100.

[18] K. Takahashi, M. Watanabe, and K. Sato, Phys. Lett. B **510**, 189 (2001).

[19] K. Takahashi, M. Watanabe, K. Sato, and T. Totani, Phys. Rev. D **64**, 093004 (2001).

[20] K. Takahashi and K. Sato, hep-ph/0110105.

[21] F. Buccella, S. Esposito, C. Gualdi, and G. Miele, Z. Phys. C **73**, 633 (1997).

[22] A. Friedland, Phys. Rev. D **64**, 013008 (2001).

[23] E. Lisi, A. Marrone, D. Montanino, A. Palazzo, and S.T. Petcov, Phys. Rev. D **63**, 093002 (2001).

[24] H. Minakata and H. Nunokawa, Phys. Rev. D **38**, 3605 (1988).

[25] S.T. Petcov, Phys. Lett. B **200**, 373 (1988).

[26] P.I. Krastev and S.T. Petcov, Phys. Lett. B **207**, 64 (1988); *erratum*, **214**, 661 (1988).

[27] L. Wolfenstein, Phys. Rev. D 17, 2369 (1978); S.P. Mikheyev and A.Yu. Smirnov, Yad. Fiz. **42**, 1441 (1985) [Sov. J. Nucl. Phys. **42**, 913 (1985)]; Nuovo Cimento C **9**, 17 (1986); V. Barger, S. Pakvasa, R.J.N. Phillips, and K. Whisnant, Phys. Rev. D **22**, 2718 (1980).

[28] G.E. Brown, H.A. Bethe, and G. Baym, Nucl. Phys. A **375**, 481 (1982).

[29] T. Shigeyama and K. Nomoto, Astrophys. J. **360**, 242 (1990).

[30] A. de Gouvea, A. Friedland, and H. Murayama, J. of High Energy Phys. **103**, 9 (2001).

[31] A. Friedland, Phys. Rev. Lett. **85**, 936 (2000).

[32] A. De Gouvea, Phys. Rev. D **63**, 093003 (2001).

[33] T.K. Kuo, J. Pantaleone, Phys. Rev. D **39**, 1930 (1989).

[34] G.L. Fogli, E. Lisi, and D. Montanino, Phys. Rev. D **54**, 2048 (1996).
[35] J. Pantaleone, Phys. Lett. B **251**, 618 (1990).
[36] G.L. Fogli, E. Lisi, D. Montanino, and A. Palazzo, Phys. Rev. D **64**, 093007 (2001).
[37] G.L. Fogli, E. Lisi, D. Montanino, and A. Palazzo, in the Proceedings of *Moriond 2001*, 36th Rencontres de Moriond on Electroweak Interactions and Unified Theories (Les Arcs, France, 2001), to appear; hep-ph/0104221.
[38] G.L. Fogli, E. Lisi, and A. Marrone, Phys. Rev. D **54**, 093005 (2001).
[39] G.L. Fogli, E. Lisi, and D. Montanino, Phys. Rev. D **49**, 3626 (1994).
[40] J. Gluza and M. Zralek, Phys. Lett. B **517**, 158 (2001).
[41] H. Minakata, H. Nunokawa, K. Shiraishi, and H. Suzuki, Mod. Phys. Lett. A **2**, 827 (1987).
[42] S.T. Petcov, Phys. Lett. B **434**, 321 (1998); M.V. Chizhov and S.T. Petcov, Phys. Rev. Lett. **83**, 1096 (1999).
[43] E.Kh. Akhmedov, Nucl. Phys. B **538**, 25 (1999).
[44] M. Fishbane, Phys. Rev. D **62**, 093009 (2000).
[45] E. Lisi and D. Montanino, Phys. Rev. D **56**, 1792 (1997).

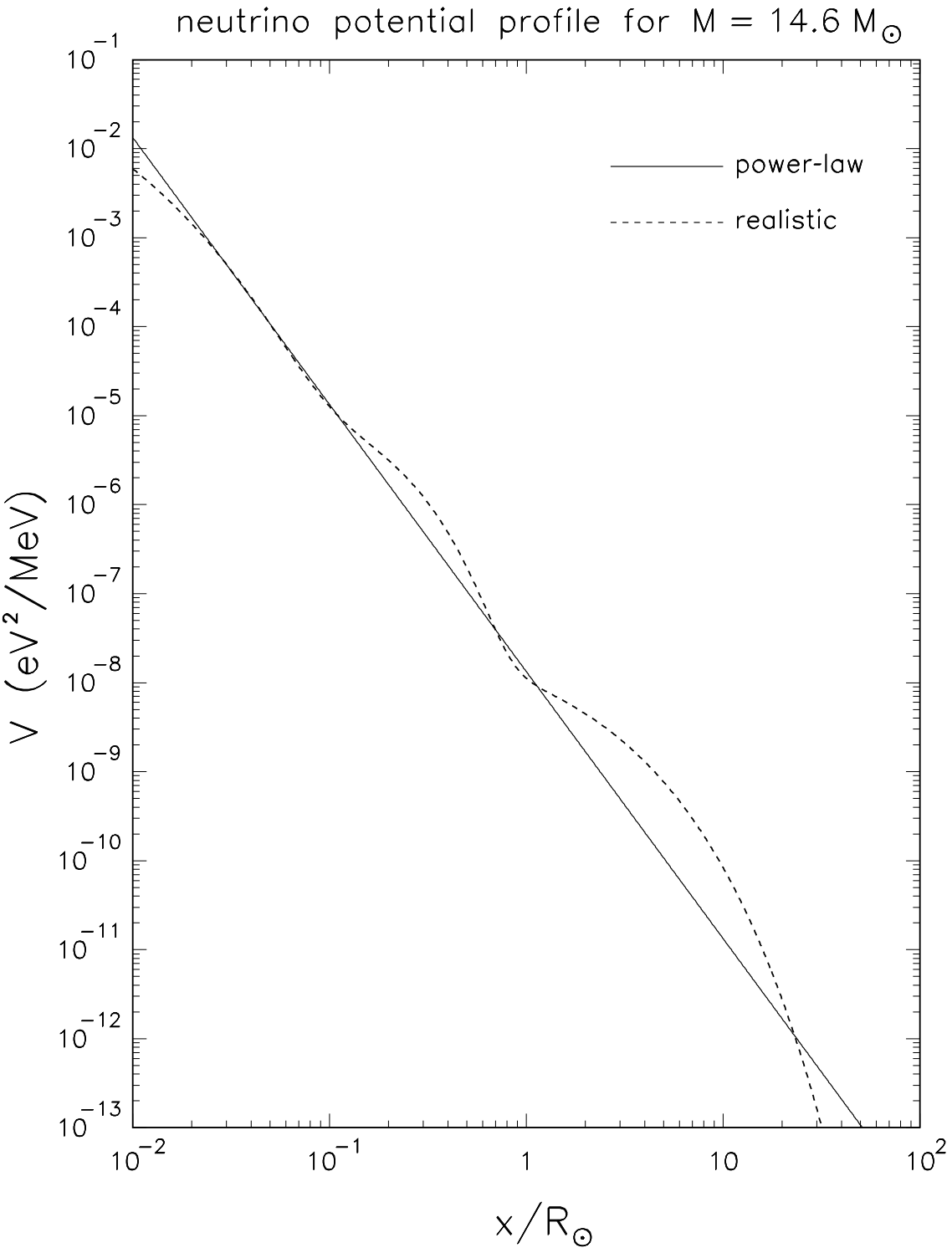

Fig. 1. Neutrino potential profiles $V(x)$ considered in this work. Dashed curve: "realistic" potential, as graphically reduced from the supernova simulation performed in [29] assuming $14.6 M_\odot$ for the ejecta. Solid line: "power-law" potential ($V \propto x^{-3}$) which best fits the realistic one.

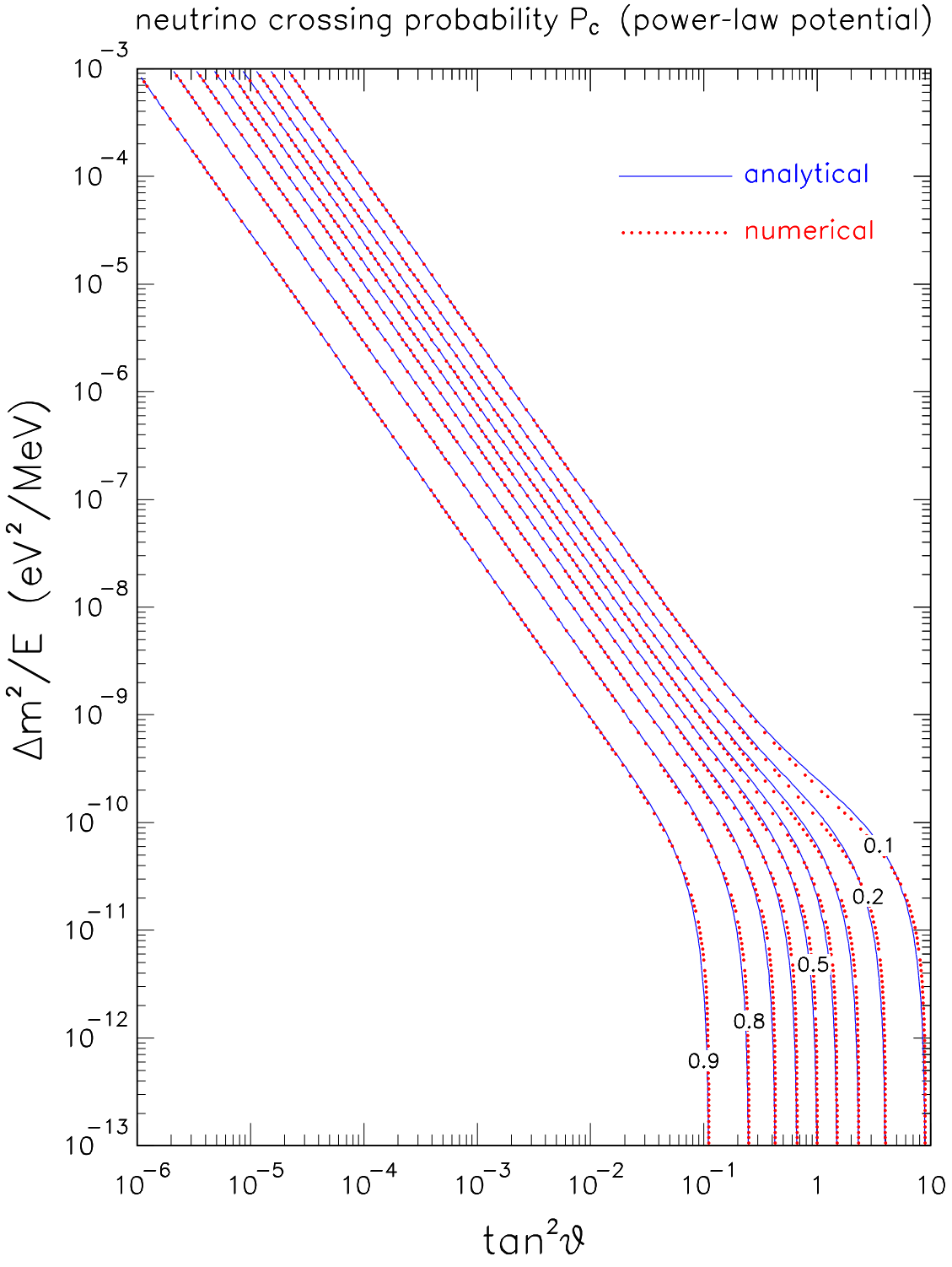

Fig. 2. Two-flavor transitions: neutrino crossing probability $P_c(\nu)$ in the parameter space $(\Delta m^2/E,\, \tan^2\theta)$ for the power-law potential profile in Fig. 1. Dotted curves: exact numerical calculations. Solid curves: results of the analytical prescription in Eqs. (12)–(14). Isolines of P_c for antineutrinos (not shown) can be obtained by reflection around the axis $\tan^2\theta = 1$. See the text for details.

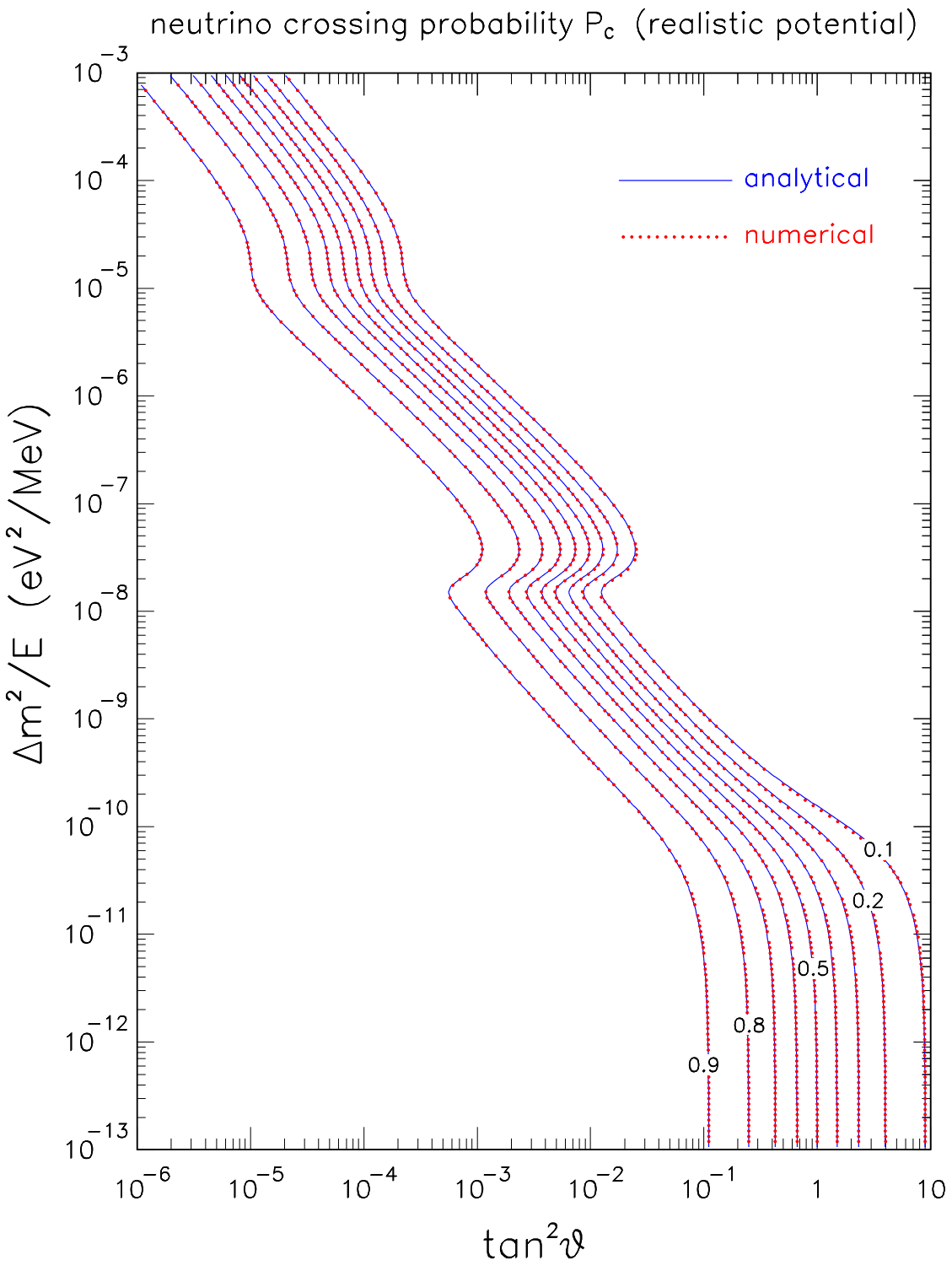

Fig. 3. As in Fig. 2, but for the realistic potential profile in Fig. 1.

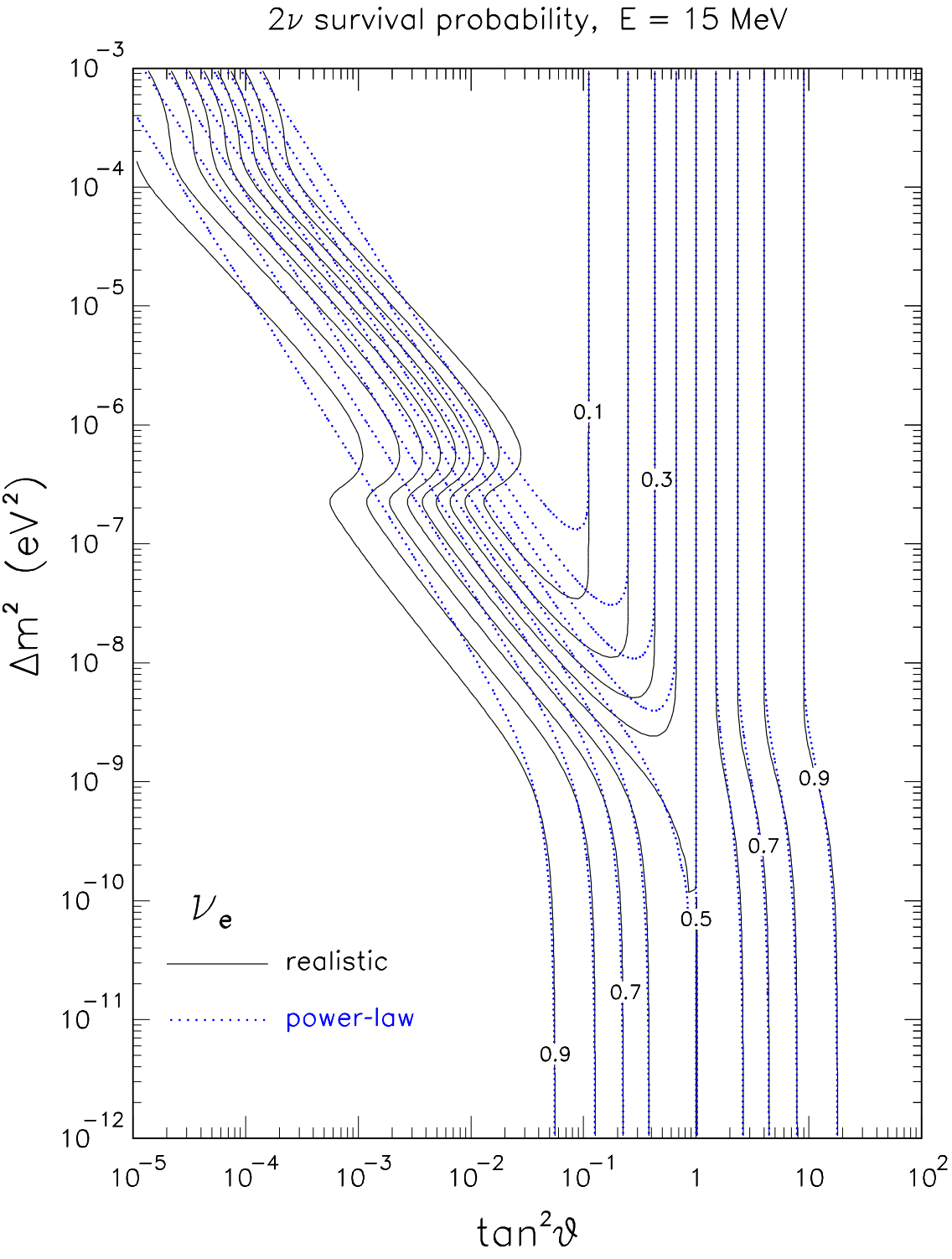

Fig. 4. Two-flavor transitions: analytical results for the electron neutrino survival probability P_{ee} in the mass-mixing plane (Δm^2, $\tan^2\theta$), at a representative neutrino energy ($E = 15$ MeV). Solid curves: realistic potential. Dotted curves: power-law potential. Isolines of P_{ee} for antineutrinos (not shown) can be obtained by reflection around the axis $\tan^2\theta = 1$. See the text for details.

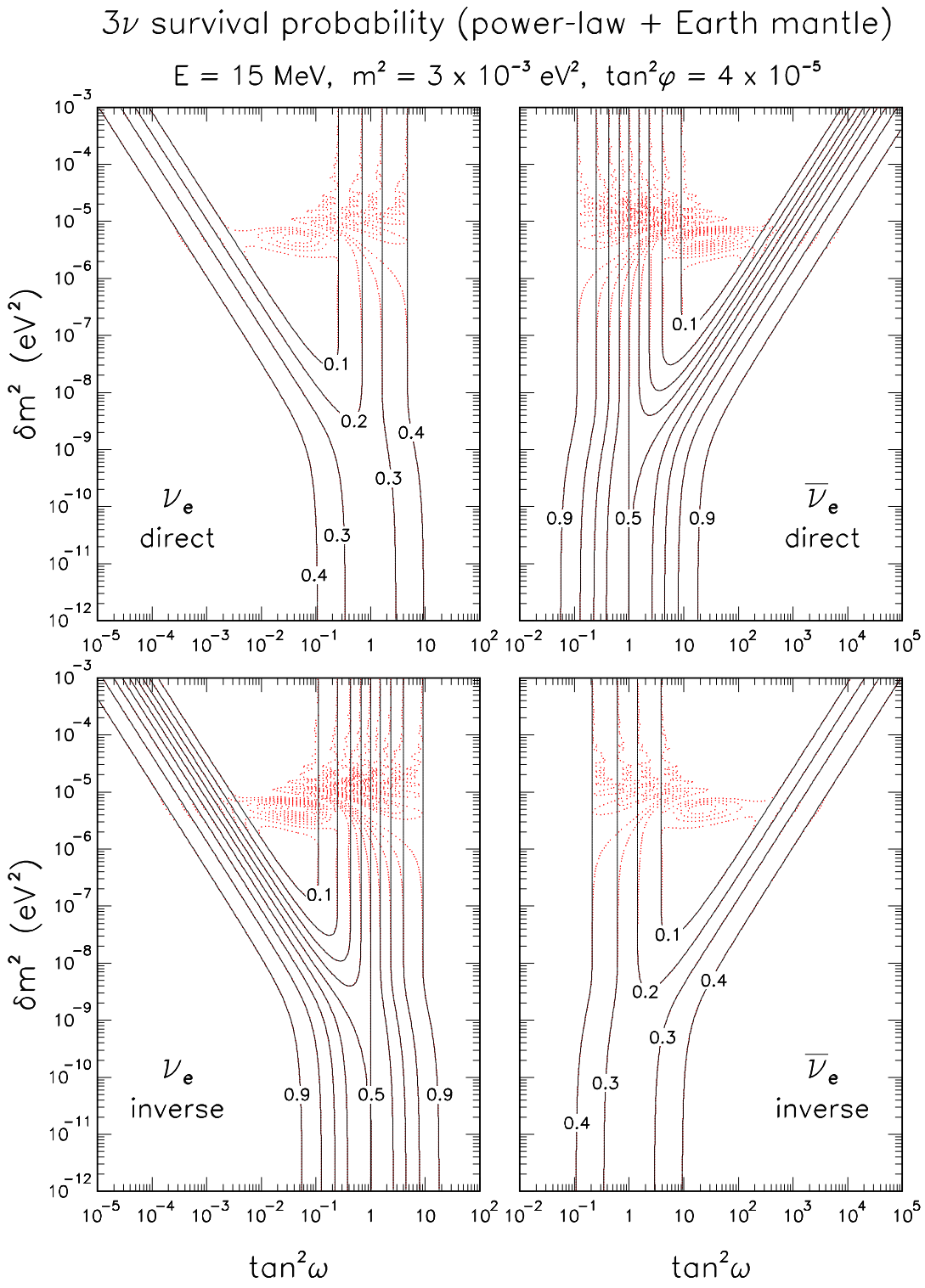

Fig. 5. Three-flavor transitions: analytical results for P_{ee} in the mass-mixing subspace (δm^2, $\tan^2\omega$), assuming the power-law profile in Fig. 1 and fixing $E = 15$ MeV, $m^2 = 3\times10^{-3}$ eV^2, and $\tan^2\phi = 4\times10^{-5}$ ($P_H^+ = 0.48$). Dotted lines include Earth matter effects for a representative path of 8500 km in the mantle (assuming $\rho = 4.5$ g/cm^3 and $Y_e = 1/2$). The upper panels refer to ν (left) and $\overline{\nu}$ (right) in the case of direct hierarchy. The lower panels refer to ν (left) and $\overline{\nu}$ (right) in the case of inverse hierarchy.